Intragenic Suppressing Mutations Correct the Folding and Intracellular Traffic of Misfolded Mutants of Yor1p, a Eukaryotic Drug Transporter

Pagant, Silvere; Halliday, John J.; Kougentakis, Christos; Miller, Elizabeth A.

Published in:
Journal of Biological Chemistry

DOI:
10.1074/jbc.M110.142760

Publication date:
2010

THE JOURNAL OF BIOLOGICAL CHEMISTRY VOL. 285, NO. 47, pp. 36304–36314, November 19, 2010

Intragenic Suppressing Mutations Correct the Folding and Intracellular Traffic of Misfolded Mutants of Yor1p, a Eukaryotic Drug Transporter*[S]

Received for publication, May 11, 2010, and in revised form, September 11, 2010 Published, JBC Papers in Press, September 13, 2010, DOI 10.1074/jbc.M110.142760

Silvere Pagant, John J. Halliday, Christos Kougentakis, and Elizabeth A. Miller[1]

From the Department of Biological Sciences, Columbia University, New York, New York 10027

ATP-binding cassette (ABC) transporters play pivotal physiological roles in substrate transport across membranes, and defective assembly of these proteins can cause severe disease associated with improper drug or ion flux. The yeast protein Yor1p is a useful model to study the biogenesis of ABC transporters; deletion of a phenylalanine residue in the first nucleotide-binding domain (NBD1) causes misassembly and retention in the endoplasmic reticulum (ER) of the resulting protein Yor1p-ΔF670, similar to the predominant disease-causing allele in humans, CFTR-ΔF508. Here we describe two novel Yor1p mutants, G278R and I1084P, which fail to assemble and traffic similar to Yor1p-ΔF670. These mutations are located in the two intracellular loops (ICLs) that interface directly with NBD1, and thus disrupt a functionally important structural module. We isolated 2 second-site mutations, F270S and R1168M, which partially correct the folding injuries associated with the G278R, I1084P, and ΔF670 mutants and reinstate their trafficking. The position of both corrective mutations at the cytoplasmic face of a transmembrane helix suggests that they restore biogenesis by influencing the behavior of the transmembrane domains rather than by direct restoration of the ICL1-ICL4-NBD1 structural module. Given the conserved topology of many ABC transporters, our findings provide new understanding of functionally important inter-domain interactions and suggest new potential avenues for correcting folding defects caused by abrogation of those domain interfaces.

ATP-binding cassette (ABC)[2] transporters comprise a large family of proteins responsible for the ATP-dependent transfer of substrates across biological membranes. Functional ABC transporters, from prokaryote to human, present a conserved architecture with two membrane-spanning domains (MSDs) linked to two cytoplasmic nucleotide-binding domains (NBDs). Important domain-domain interfaces govern the quaternary structure of ABC transporters and participate in the conformational changes required for their regulated function as membrane transporters (1). The substrate binding pocket and translocation channel across the lipid bilayer are formed by specific interactions among the multiple transmembrane helices (TMHs) that comprise the two MSDs. Similarly, two composite ATP binding pockets are shaped by the interface between two cytoplasmic NBDs (2–8). The strength of these two interfaces is illustrated by the fact that bacterial multidrug ABC proteins are generally expressed as "half-transporters" that contain one MSD fused to one NBD, which dimerize to form a full transporter. This diverse family of proteins encompasses variants that act as either exporters or importers, and that transport diverse molecules, including ions, polysaccharides, vitamins, lipids, and peptides, yet all share these two general and fundamental interfaces (1).

The recent crystal structures of ABC transporters reveal that intracellular loops (ICLs), which extend into the cytoplasm from the MSDs, contain short helices oriented roughly parallel to the plane of the membrane that create an interface between NBDs and MSDs. This interface is thought to be essential in coupling the information of ATP binding and hydrolysis to ligand translocation, as shown by the studies conducted on the human TAP transporter (9) and on the yeast drug pump Pdr5 (10). However, despite the conserved nature of this interface, the precise mode of interaction differs according to the type of transport: in the bacterial importers BtuCD and ModBC, the ICL-NBD interface is composed entirely of interactions within the same half-transporter (11, 12), whereas in the bacterial exporters Sav1866 and MsbA, the two halves of the transporter undergo domain swapping such that the ICLs of one polypeptide interact predominantly with the NBD of the opposite half-transporter (13, 14). A similar domain-swapped arrangement is also observed in the structure of a eukaryotic full transporter, P-glycoprotein (15), and likely applies to other eukaryotic exporters, as determined by *in vivo* cross-linking (16–19). Further characterization of the architecture of specific ABC transporters is of particular interest in gaining a better understanding of the common mechanisms involved in the function of ABC transporters and the molecular determinants governing the specificity and directionality of transport.

Detailed comprehension of how cells handle ABC transporters during their biogenesis also has important implications for human health because many mutations that cause misfolding

* This work was supported, in whole or in part, by National Institutes of Health Grant GM078186 (to E. A. M.) and Cystic Fibrosis Foundation Grant PAGANT08F0 (to S. P.).

[S] The on-line version of this article (available at http://www.jbc.org) contains supplemental Table S1 and Figs. S1–S3.

[1] To whom correspondence should be addressed: 617A Fairchild Center, M.C. 2264, New York, NY 10027. Tel.: 212-854-2264; Fax: 212-865-8426; E-mail: em2282@columbia.edu.

[2] The abbreviations used are: ABC, ATP-binding cassette; CFTR, cystic fibrosis transmembrane conductance regulator; ER, endoplasmic reticulum; MSD, membrane spanning domain; NBD, nucleotide-binding domain; TMH, transmembrane helix; ICL, intracellular loop; M2M, 1,2-ethanediyl bismethanethiosulfonate; M5M, 1,5-pentanediyl bismethanethiosulfonate; M8M, 3,6-dioxaoctane-1,8-diyl bismethanethiosulfonate; ERQC, ER quality control; ERAD, ER-associated degradation.

events in ABC transporters have been linked to several hereditary diseases. Cystic fibrosis (CF) represents a classical example of a loss-of-function disease related to ABC transporter function: CF-causing mutations are associated with impaired assembly of the cystic fibrosis transmembrane conductance regulator (CFTR), an ABC transporter that controls chloride flux across the plasma membrane (20). Many mutations in CFTR create aberrant proteins that are retained in the endoplasmic reticulum (ER) because of their recognition by the ER quality control process that prevents deployment of misfolded proteins (21–23). Similarly, individual differences in therapeutic drug response or diseases such as sitosterolemia, and progressive familial intrahepatic cholestasis type 3 (PFIC3) have been associated with the misassembly and ER retention of ABCG2 (24, 25), ABCG5/8 (26, 27), and ABCB4 (28), respectively. However, the exact nature of the folding lesions that trigger the quality control checkpoint remains poorly understood. Thus, comprehensive characterization of the folding defect(s) induced by disease-related mutations on the quaternary structure of ABC transporters may provide insight into the potential for correction via the design of novel therapeutic strategies.

We have developed Yor1p, a yeast ABC transporter, as a model to study the relationship between protein assembly and trafficking in *Saccharomyces cerevisiae* (18, 29). Yor1p functions at the plasma membrane as a drug pump to clear toxic substances from the cytosol, and is required for growth in the presence of the mitochondrial poison, oligomycin. Using *in vivo* cysteine cross-linking to probe for specific domain-domain interactions that contribute to its native conformation, we showed that Yor1p shares the same quaternary architecture as CFTR and P-glycoprotein, with domain swapping creating two structural modules: ICL1-ICL4-NBD1 and ICL2-ICL3-NBD2 (18). Yor1p-ΔF670, which contains a deletion of a phenylalanine residue within NBD1, equivalent to most prevalent disease-related allele of CFTR, loses these inter-domain contacts and is instead misfolded, retained in the ER, and degraded by ER-associated degradation (ERAD), similar to CFTR-ΔF508 (29). In contrast, a different disease-related substitution, R387G, which likely perturbs the ICL2-ICL3-NBD2 module, generates an aberrant form of Yor1p that is localized correctly to the plasma membrane (18). Therefore, the yeast ER quality control (ERQC) system seems to sense different aberrant conformations within the same protein. To gain more insight into the nature of folding disruptions detected by QC and the inter-domain arrangements required for functionality, we characterized two additional processing mutations predicted to primarily affect the ICL1-ICL4-NBD1 module. In addition, we identified 2 second-site mutations that rescue the folding and the trafficking of these aberrant proteins, likely through stabilization of the hydrophobic transmembrane domains. Our findings suggest that multiple modes of rescue of aberrant ABC transporters are possible.

EXPERIMENTAL PROCEDURES

Yeast Strains and Media—Cultures were grown at 30 °C in standard rich medium (YPD: 1% yeast extract, 2% peptone, and 2% glucose) or synthetic complete medium (SC: 0.67% yeast nitrogen base and 2% glucose, supplemented with amino acids appropriate for auxotrophic growth). For testing sensitivity to oligomycin, strains were grown to saturation, and then 10-fold serial dilutions were applied to YPEG plates (1% yeast extract, 2% peptone, 3% ethanol, and 3% glycerol) supplemented with oligomycin (Sigma).

Plasmids—The plasmids used in this study are listed in supplemental Table S1. pEAE83 bearing *YOR1-HA* in pRS316 was a gift from Scott Moye-Rowley (University of Iowa). This plasmid was the basis for site-directed mutagenesis by using QuikChange mutagenesis (Stratagene, La Jolla, CA) to obtain various hemagglutinin (HA)-tagged Yor1p mutants used in this study. pEAE93 was a gift from Scott Moye-Rowley and contains an in-frame fusion of green fluorescent protein (GFP) to the C terminus of Yor1p.

Intragenic Suppressor Screen for Rescue of Yor1-I1084P—A plasmid bearing *yor1-I1084P*, marked by the *URA3* gene, was mutagenized using *Escherichia coli* strain XL1Red. Mutagenized plasmid DNA was introduced by standard LiAc transformation into a Δ*yor1* strain. Transformants were replica-plated onto yeast medium that contained 0.2 mg/liter of oligomycin. Oligomycin-resistant strains in which extragenic mutations, perhaps in mitochondrial genes or other drug exporters, may have contributed to oligomycin resistance independent of Yor1p function were eliminated by growing candidates on medium containing 5-fluoroorotic acid, which is toxic in the presence of the *URA3* gene product and, thereby, compels the yeast cells to lose the plasmid containing *yor1-I1084P*. Cells that remained oligomycin resistant even in the absence of any *YOR1*-containing plasmid following 5-fluoroorotic acid treatment were discarded. Conversely, sensitivity to oligomycin after treatment by 5-fluoroorotic acid indicated that oligomycin resistance of the original suppressor was dependent on the *yor1-I1084P* plasmid. As further confirmation, these plasmids were recovered and retransformed into a new Δ*yor1* strain to verify their ability to confer oligomycin resistance. The entire *YOR1* gene was sequenced in the validated plasmids to identify the suppressing mutation. As a final control, the suppressing mutation was reintroduced by site-directed mutagenesis into an intact *yor1-I1084P* plasmid, which was retransformed into a new Δ*yor1* strain to confirm the oligomycin-resistant phenotype.

Cross-linking and Limited Proteolysis—Domain-domain interactions were probed using cysteine-reactive cross-linking as described previously (18). Briefly, spheroplasts of cells expressing cysteine mutants of Yor1p-HA were incubated with 1,2-ethanediyl bismethanethiosulfonate (M2M), 1,5-pentanediyl bismethanethiosulfonate (M5M), or 3,6-dioxaoctane-1,8-diyl bismethanethiosulfonate (M8M) (Toronto Research Chemicals, North York, ON, Canada). Cells were cross-linked for 15 min at room temperature, then collected by centrifugation and resuspended in 100 μl of 1% SDS prior to addition of 50 μl of 3× SDS sample buffer without reducing agent. Cells were lysed, and proteins were solubilized by heating to 55 °C for 5 min, and separated by non-reducing SDS-PAGE, transferred to polyvinylidene difluoride, and analyzed by immunoblot analysis using anti-HA antibodies (Covance, Princeton, NJ).

Global protein folding was tested using limited proteolysis by exposing membranes or semi-intact cells to increasing concen-

trations of trypsin as described previously (18). Spheroplasts of cells expressing different alleles of Yor1p-HA were resuspended in 100 μl of 20 mM HEPES, pH 7.4, and divided into four 25-μl reactions (2.5 A_{600}/reaction). Each reaction was treated with final concentrations of 0, 25, 50, or 100 ng/μl of trypsin (Sigma) for 10 min on ice. Digestion was terminated by addition of 0.2 μg/ml (final concentration) of soybean trypsin inhibitor (Sigma) to all reactions and incubated on ice for 15 min. Proteins were separated by SDS-PAGE, transferred to polyvinylidene difluoride, and the pattern of Yor1p fragments analyzed by immunoblot by using an anti-HA antibody.

In Vitro Vesicle Formation—The ability of Yor1p to be captured into ER-derived vesicles was tested using radiolabeled permeabilized cells incubated with purified COPII coat proteins as previously described (29). Semi-intact cells expressing different forms of Yor1p-HA were radiolabeled as described previously (29). Radiolabeled semi-intact cells were then lysed by being washed once with low acetate B88 (20 mM HEPES, pH 6.8, 250 mM sorbitol, 50 mM potassium acetate, and 5 mM magnesium acetate) and twice with B88. Semi-intact cells were then incubated with COPII proteins (10 μg/ml of Sar1p, 10 μg/ml of Sec23p/24p, and 20 μg/ml of Sec13/31p) either in the presence of 0.1 mM GTP with a 10× ATP regeneration system or 0.1 mM GDP. Vesicles generated were separated from donor membranes by centrifugation at 16,000 × *g* for 30 min, solubilized with 1% SDS (final concentration), and diluted with immunoprecipitation buffer (50 mM Tris, pH 7.5, 160 mM NaCl, 1% Triton X-100, and 2 mM NaN_3). Proteins were first immunoprecipitated using monoclonal anti-HA antibodies (Covance) precoupled to protein G-Sepharose beads (GE Healthcare). Subsequent to the HA immunoprecipation the same vesicle fractions were immunoprecipitated using polyclonal antibodies against Sec22p coupled to protein A-Sepharose beads (GE Healthcare). Immune complexes were separated by SDS-PAGE and analyzed by phosphorimage analysis using a Storm PhosphorImager (GE Healthcare). Proteins were quantified using ImageQuant software (GE Healthcare).

Pulse-Chase Analysis of Yor1p Stability—Cells were grown to mid-log phase in complete synthetic medium, and then harvested, resuspended in fresh medium lacking methionine/cysteine, and incubated for 15 min with gentle shaking at 30 °C. Cells were metabolically labeled for 7 min by adding 30 μCi of Express protein labeling mixture (MP Biomedicals) per A_{600} unit of cells. A 10× chase solution (10 mM L-cysteine, 50 mM L-methionine, 4% yeast extract, and 2% glucose) was added and 2 OD aliquots of cells were harvested at different times. At each time point, cells were transferred to chilled tubes, and sodium azide was added to a final concentration of 20 mM. Cells were washed once with 20 mM sodium azide and resuspended in 100 μl of 1% SDS. Glass beads were added, and cells were lysed by vortexing for 15 min at 4 °C. Cell lysates were heated at 55 °C for 5 min, diluted with 5 volumes of immunoprecipitation buffer (50 mM Tris, pH 7.5, 160 mM NaCl, 1% Triton X-100, and 2 mM NaN_3), and cleared by centrifugation. Yor1p was immunoprecipitated from the cleared lysate and analyzed by SDS-PAGE and phosphorimage analysis as described above.

Live Cell Imaging—Strains expressing different variants of Yor1p-GFP were grown in selective medium to mid-log phase and imaged using an Olympus IX81-FV500 Confocal microscope with a ×100 (1.4NA) objective. Images were collected with IPLab 4.0 and analyzed using Adobe Photoshop (Adobe Systems, Mountain View, CA).

RESULTS

R378G (ICL1) and I1084P (ICL4) Induce Folding Lesions Detected by ERQC—The hypothesis that the formation of an ICL1-ICL4-NBD1 module may play a critical role in generating the quaternary assembly that is compatible with ER egress is supported by the observation that numerous CF-associated mutations that map to ICL1 and ICL4 of CFTR cause ER retention (21–23). We selected two mutations (G149R, located at the start of ICL1, and L1065P, located in ICL4 and predicted to participate directly in the NBD1-ICL4 interface) and introduced the equivalent mutations into Yor1p (Fig. 1*A*): Yor1p-G278R and Yor1p-I1084P, respectively. The different *yor1-ICL* mutants were introduced into cells where the chromosomal copy of *YOR1* had been deleted to test their ability to confer oligomycin resistance (Fig. 1*B*). Like *yor1-ΔF670*, expression of either *yor1-G278R* or *yor1-I1084P* was unable to permit growth in the presence of oligomycin, whereas wild-type *YOR1* conferred strong survival in the presence of the drug. These data suggest that the function and/or the trafficking of Yor1p is impaired by both mutations. We first investigated whether oligomycin sensitivity of these *yor1-ICL* mutants was caused by misfolding of the proteins, as is the case for Yor1p-ΔF. We subjected membranes containing either wild-type or mutant Yor1p to limited proteolysis by exposing permeabilized cells to increasing concentrations of trypsin. The susceptibility of Yor1p to degradation was analyzed by immunoblotting: wild-type Yor1p presented a persistent ~160-kDa band and a single major cleavage product of ~60 kDa with increasing amounts of trypsin (Fig. 1*C, left panel*), whereas Yor1p-ΔF670 was readily converted to a number of smaller cleavage products. This increased susceptibility to proteolysis likely derives from exposure of additional trypsin cleavage sites within the aberrant conformation of Yor1p-ΔF670. Interestingly, Yor1p-G278R and Yor1p-I1084P showed a similar cleavage pattern to that of Yor1p-ΔF670 (Fig. 1*C*), suggesting that the three different mutants share a destabilized quaternary structure. As a separate assay to inspect how the different mutations might affect folding and assembly of Yor1p, we made use of cysteine cross-linking between the 6th (Leu-479) and 12th (Leu-1162) TMH domains of Yor1p, previously developed to probe the MSD-MSD interface (29). Membranes expressing wild-type Yor1p that contained cysteine substitutions at Leu-479 (TMH6) and Leu-1162 (TMH12) were exposed to a methanethiosulfonate cross-linker M8M and the mobility of the protein monitored by non-reducing SDS-PAGE and anti-HA immunoblotting. As shown previously, on exposure to cross-linker, a species with reduced mobility, likely corresponding to a cross-linked product, was detected for wild-type Yor1p (Fig. 1*D*). After introduction of G278R and I1084P mutations, no cross-linked species were detected; instead, the unmodified protein disappeared and the majority of the protein presented as a very high molecular weight aggregate that largely failed to enter the resolving gel. Similar higher order aggregation was also detected for

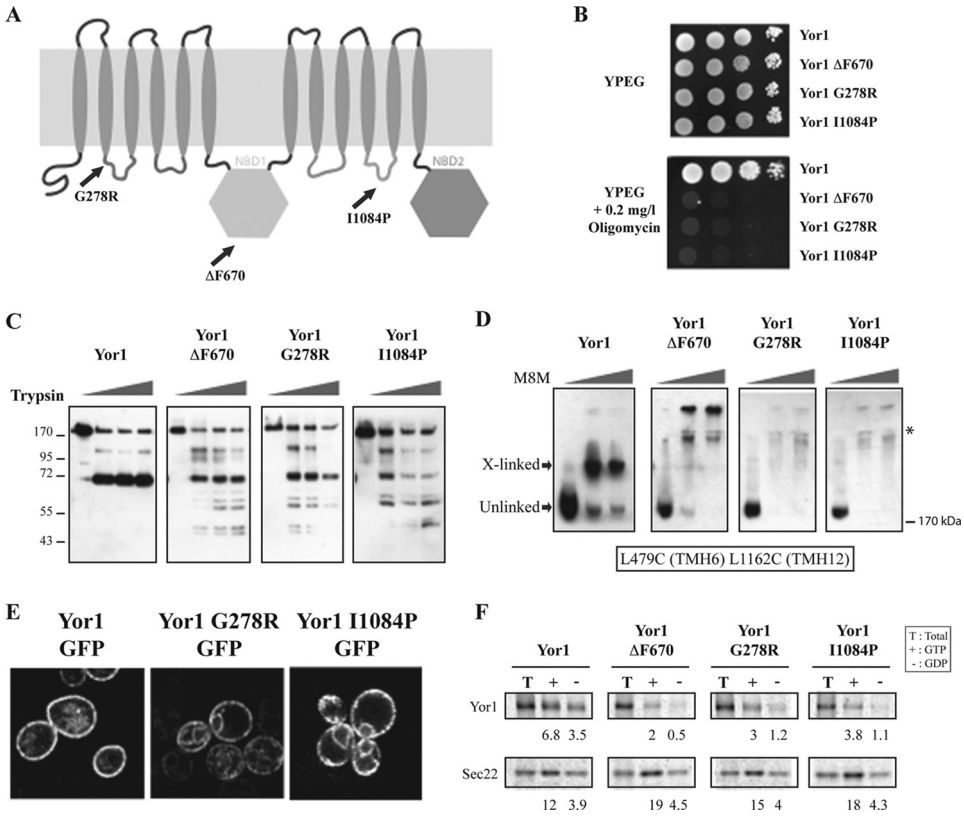

FIGURE 1. **G278R (ICL1) and I1084P (ICL4) mutations impair the biogenesis of Yor1p.** *A*, schematic map of processing mutations in Yor1p. *B*, the effect of mutations on Yor1p function was tested by complementation of the drug sensitivity of *yor1*Δ. Transformants were spotted onto YPEG or YPEG supplemented with oligomycin (10-fold serial dilutions). Plasmids *yor1-ΔF670, yor1-G278R*, and *yor1-I1084P* confer loss of function. *C*, permeabilized cells expressing HA-tagged forms of Yor1p were subjected to limited proteolysis by treating membranes with increasing amounts of trypsin followed by SDS-PAGE and immunoblotting to detect HA-tagged proteolytic fragments. The ΔF670, G278R, and I1084P variants show increased sensitivity to proteolysis compared with that observed for wild-type Yor1p. *D*, membranes expressing HA-tagged forms of cysteine-substituted Yor1p designed to probe the proximity of TMH6 (L479C) and TMH12 (L1162C) were cross-linked with increasing concentrations of M8M. Yor1p-ΔF670, Yor1p-G278R, and Yor1p-I1084P failed to produce the cross-linked species observed for the wild-type protein. *Asterisk* marks the interface between stacking and resolving gels. *E*, cells expressing Yor1p-GFP fusions were examined by fluorescence microscopy. Yor1p-G278R and Yor1-I1084P show perinuclear ER staining, unlike Yor1p that localizes exclusively at the plasma membrane. *F*, permeabilized cells from cells expressing HA-tagged forms of Yor1p were used in an *in vitro* vesicle budding assay. Yor1p-ΔF670, Yor1p-G278R, and Yor1p-I1084P showed reduced incorporation into COPII vesicles compared with Yor1p. Total membranes (*T*) and budded vesicles were collected from reactions that contained either GTP (+) or GDP (−), and consecutively immunoprecipitated using anti-HA antibodies and anti-Sec22 antibodies. Yor1p and Sec22p packaging into vesicles was quantified by immunoprecipitation followed by SDS-PAGE and phosphorimage analysis. *Numbers below* the individual experiments represent the budding efficiency as a percentage of the total protein for one representative experiment. Statistical analysis of at least three independent experiments is represented under supplemental Fig. S1*A*.

Yor1p-ΔF, and is thought to represent nonspecific cross-linking of exposed cysteine residues that would normally be buried in the correctly assembled structure. Thus, the strong oligomycin sensitivity presented by these three mutants (Yor1p-G278R, Yor1p-ΔF670, and Yor1p-I1084P) can be correlated with significant and comparable injury to the native conformation of Yor1p.

To examine if the folding injury inflicted by the ICL mutations results in ER retention, as is the case for Yor1p-ΔF, we examined localization of GFP-tagged fusions of the various forms of Yor1p. Whereas wild-type Yor1p was exclusively observed at the plasma membrane, the two new ICL mutants showed strong perinuclear localization, consistent with impaired trafficking out of the ER (Fig. 1*E*). To quantify the degree of ER retention of the misfolded mutants, we used an *in vitro* vesicle budding assay that recapitulates COPII vesicle formation from radiolabeled permeabilized cells (semi-intact cells). Cells expressing an HA-tagged copy of either wild-type Yor1p or the Yor1p-ICL mutants were pulse-labeled, converted to spheroplasts, and permeabilized prior to incubation with the COPII components, Sar1p, Sec23p/Sec24p, and Sec13p/Sec31p in the presence of either GTP or GDP. This incubation drives the *in vitro* formation of transport vesicles, which can be separated from donor membranes by differential centrifugation, and the specific capture of cargo proteins into vesicles was quantified by immunoprecipitation and phosphorimaging. As previously shown, wild-type Yor1p was efficiently packaged into COPII vesicles, whereas Yor1p-ΔF was detected at much lower levels in the vesicle fraction, illustrating that the mutant protein has engaged the ER quality control checkpoint that prevents ER export of aberrant cellular proteins (Fig. 1*F* and supplemental Fig. S1*A*). Similarly, Yor1p-G278R and Yor1p-I1084P were largely absent from the vesicle fraction, consistent with their retention in the ER (Fig. 1*F* and supplemental Fig. S1*A*). As a control to measure vesicle release, the ER-Golgi SNARE protein, Sec22p, was immunoprecipitated from the unbound supernatant fraction resulting from the initial anti-HA immunoprecipitation. In each case, Sec22p was efficiently captured into COPII vesicles, indicating that defective packaging of the Yor1p mutants is specific to the altered protein. Taken together these data illustrate that the G278R (ICL1) and I1084P (ICL4) mutations create folding lesions that trigger detection by ERQC, and might suggest that establishment of a stable ICL1-ICL4-NBD1 module is a determinant in the acquisition of the quaternary structure appropriate for ER exit.

Isolation of Intragenic Suppressors of yor1-I1084P—We sought to gain more information about the folding lesion responsible for ER retention by screening for intragenic suppressors of ER-retained mutants of Yor1 using the oligomycin sensitivity associated with these mutants. We hoped to isolate secondary substitutions in the protein that would induce a structural change to compensate for the folding deficiency of the processing mutant forms of Yor1p.

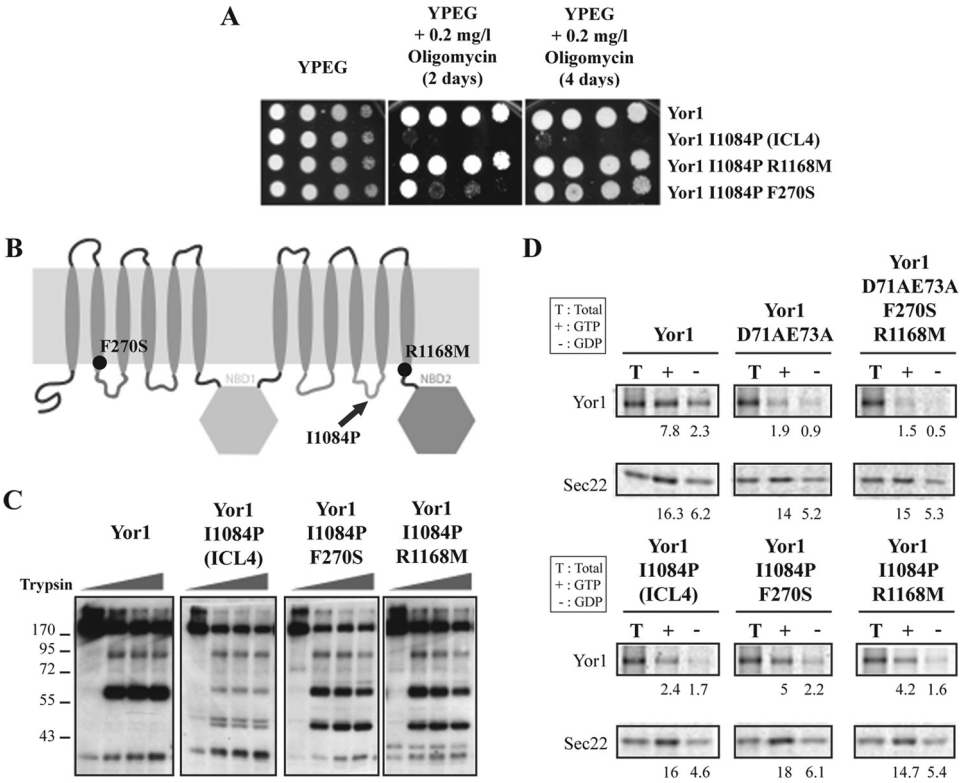

FIGURE 2. **Intragenic suppressors of Yor1p-I1084P.** *A*, phenotypic characterization of the suppressing mutations to rescue the function of Yor1-I1084P. A strain bearing a deletion in *YOR1* was transformed with plasmids expressing the alleles indicated and 10-fold serial dilutions spotted onto YPEG or YPEG supplemented with oligomycin. *B*, schematic map of mutations that suppress the oligomycin sensitivity of Yor1-I1084P. *C*, the effect of the second-site mutations on the folding lesions presented by Yor1p-I1084P was analyzed by trypsin digest. Suppressing mutations F270S and R1168M were able to partially correct the aberrant conformation of Yor1p-I1084P. *D*, the effect of the corrective mutations on ER retention presented by Yor1p-I1084P was analyzed using an *in vitro* COPII vesicle budding assay, as described in the legend to Fig. 1. Suppressing mutations F270S and R1168M were able to partially correct the incorporation of Yor1p-I1084P into COPII vesicles, but were inefficient in suppressing the ER retained mutant D71A/E73A. Statistical analysis of at least three independent experiments is represented under supplemental Fig. S1*B*.

Previous attempts using intragenic suppressor screens of Yor1p-ΔF were limited in their success in identifying substitutions that conferred oligomycin resistance: only a single mutation was isolated and this alteration did not rescue folding or ER export of Yor1-ΔF. Instead, this new mutation likely conferred a gain-of-function to the small fraction of Yor1p-ΔF that escaped ER quality control.[3] We hypothesized that the use of Yor1p-G278R or Yor1p-I1084P would be more proficient than Yor1p-ΔF in the isolation of suppressing mutations, in part because only the ICL1-ICL4-NBD1 module is predicted to be affected by each of these mutations, whereas ΔF670 also ablates the NBD1-NBD2 interface.

A plasmid bearing *yor1-I1084P* was mutagenized and introduced into a Δ*yor1* strain, and transformants that conferred oligomycin resistance were selected. Plasmids from oligomycin-resistant colonies were recovered, and *YOR1* was sequenced to identify the suppressing mutation. As a final control, any suppressing mutations were reintroduced into a *yor1-I1084P* plasmid by site-directed mutagenesis, and subsequently introduced anew into a Δ*yor1* strain to confirm the oligomycin-resistant phenotype. After screening ~300,000 independent transformants, we identified two substitutions (F270S and R1168M) that independently rescued the oligomycin sensitivity of *yor1-I1084P* (Fig. 2*A*). R1168M, located at the junction of TMH12 and NBD2 (Fig. 2*B*) showed a stronger effect than F270S, located at the end of TMH2, because *yor1-I1084P/R1168M* presented strong growth in the presence of oligomycin after only 2 days, whereas the effect of F270S required a longer incubation.

We expected the suppressing mutations to rescue the folding defect associated with the original I1084P mutation. We tested this by assessing the sensitivity of Yor1p to trypsinolysis. Yor1p-I1084P/F270S and Yor1p-I1084P/R1168M both displayed similar trypsin digest profiles, with two major cleavage products of ~60 and ~40 kDa (Fig. 2*C*). This pattern seems to represent an intermediate state between wild-type Yor1p, which only exhibits the ~60-kDa product, and Yor1p-I1084P, which accumulates smaller fragments. These data suggest that the suppressing mutations are able to partially rescue the assembly defect caused by the I1084P lesion. Interestingly, both F270S and R1168M mutations seem to have a similar effect on the folding of Yor1p despite the difference in degree of oligomycin resistance that they confer when combined with the I1084P allele. In addition, pulse-chase experiments show that each suppression causes a small but significant increase of the half-life of Yor1p-I1084P (supplemental Fig. S2).

Finally, we examined if this partial restoration of folding was sufficient to rescue the incorporation of Yor1p-I1084P into COPII vesicles. The use of the quantitative *in vitro* vesicle budding assay revealed that Yor1p-I1084P/F270S and Yor1p-I1084P/R1168M populated COPII vesicles at intermediate levels relative to that exhibited by Yor1p-I1084P (Fig. 2*D* and supplemental Fig. S1*B*). Taken together, these data suggest that the folding rescue conferred by F270S and R1168M, although incomplete, is sufficient to at least partially bypass the quality control checkpoint. Moreover, we used the same assay to investigate if these suppressing mutations are able to influence the uptake of Yor1-D71A/E73A into ER-derived vesicles. Previous characterization of this Yor1p variant showed that D71A/E73A constitutes a diacidic motif, exposed in the cytosol, which acts as the ER exit signal for Yor1p (32). Therefore, the resulting protein Yor1-D71A/E73A shows a limited ability to traffic out of the ER despite no detectable folding defect. Interestingly, F270S and R1168M, even added concurrently, failed to improve the inclusion of Yor1-D71A/E73A in ER-derived vesicles (Fig.

[3] R. Louie and E. A. Miller, unpublished data.

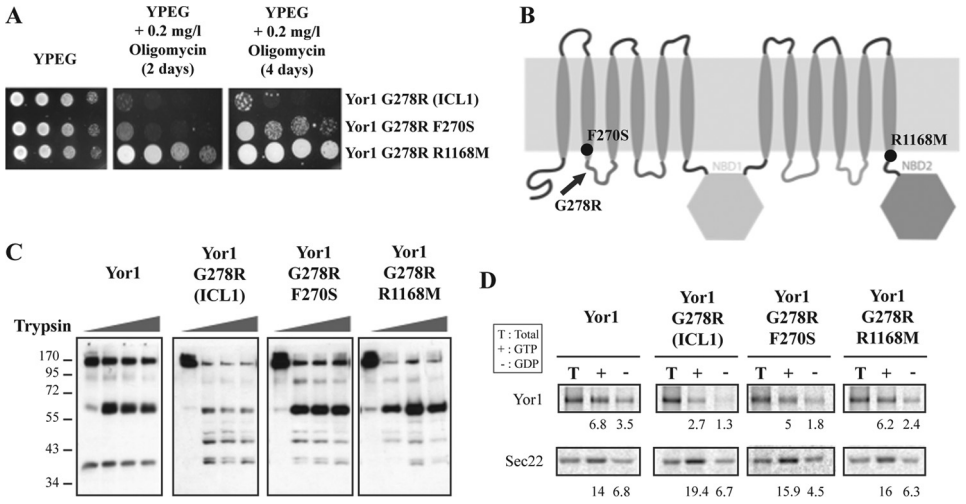

FIGURE 3. **Intragenic suppressors F270S and R1168M correct the biogenesis of Yor1p-G278R.** *A*, the capacity of suppressing mutations to rescue the function of G278R was tested *in vivo* by assessing growth in the presence of oligomycin. The plasmids encoding the alleles indicated were transformed into a Δ*yor1* strain and 10-fold serial dilutions were spotted onto YPEG or YPEG supplemented with oligomycin. *B*, schematic map of the mutations used in Fig. 3. *C*, the effect of the suppressing mutations on the folding lesions presented by Yor1p-G278R was analyzed by limited proteolysis. The defective assembly of Yor1p created by G278R was partially corrected by F270S and R1168M. *D*, an *in vitro* COPII vesicle budding assay was used, as described in the legend to Fig. 1, to monitor the capacity of the suppressing mutations to alleviate the ER retention presented by Yor1p-G278R. Yor1p-G278R/F270S and Yor1p-G278R/R1168M showed higher incorporation into ER-derived vesicles compared with Yor1-G278R. Statistical analysis of at least three independent experiments is represented under supplemental Fig. S1*C*.

2*D*). This result corroborates the idea that the suppressing mutations restore the capacity of I1084P to exit the ER because of their compensatory action on Yor1p folding and not due to a more general effect on the process leading to the capture of Yor1 into COPII vesicles.

F270S and R1168M Suppress the Defects Caused by G278R (ICL1) and ΔF (NBD1)—We reasoned that mutations that suppress the biogenesis defect caused by I1084P might also be able to rescue other ER-retained alleles of Yor1p, especially those that have defects in the formation of the ICL1-ICL4-NBD1 module similar to Yor1p-I1084P. We first tested rescue of the G278R mutant and observed restoration of oligomycin resistance by both F270S and R1168M mutations (Fig. 3*A*). Interestingly, stronger drug resistance was associated with the R1168M suppression relative to the F270S allele, similar that that seen in the Yor1p-I1084P context. Using limited proteolysis we could correlate the phenotypic rescue conferred by F270S and R1168M with a significant restoration of the defective assembly of Yor1p-G278R (Fig. 3*C*): in each case the suppressed mutants showed a major cleavage product of ~60 kDa, similar to that of wild-type Yor1p, but also showed additional minor cleavage products of smaller size similar to those observed for Yor1p-G278R. Therefore, the conformation of the two reverted proteins likely represents an intermediate folding state between a native conformation and the relaxed assembly induced by the G278R allele. Furthermore, the architecture shared by Yor1p-G278R/F270S and Yor1p-G278R/R1168M is probably distinct from the one exhibited by Yor1p-I1084P/F270S and Yor1p-I1084P/R1168M because the predominant cleaved product of ~40 kDa observed for the suppressed YorI1084P variants (Fig. 2*C*) could not be detected for the suppressed Yor1p-G278R mutants. This diversity in trypsin profiles might indicate a subtle distinction in the mechanism by which the suppressing mutations correct the two different aberrant mutants. Conversely, alterations in Yor1p-ICL1 and Yor1p-ICL4 might induce two different conformations that can be revealed only in combination with the suppressing mutations. In any case, the rescue of folding conferred by F270S and R1168M in the context of Yor1p-G278R is sufficient to restore its incorporation into COPII vesicles (Fig. 3*D* and supplemental Fig. S1*C*).

We next investigated if the suppressing mutations could rescue the injury caused by ΔF; although this lesion is located in NBD1, it also seems to affect formation of the ICL1-ICL4-NBD1 module and additionally interferes with the creation of an interface between NBD1 and NBD2. The introduction of either F270S or R1168M into Yor1p-ΔF showed little to no suppression of oligomycin sensitivity even at very low drug doses (0.1 μg/ml) (Fig. 4*A*). However, when both suppressing mutations were incorporated simultaneously, Yor1p-ΔF/F270S/R1168M displayed substantial growth on 0.2 μg/ml of oligomycin (Fig. 4*A*). These data seem to confirm the hypothesis that ΔF causes a more severe folding defect than the ICL mutations, and that the combinatorial effect of F270S and R1168M is necessary to rescue this specific conformation. In support of this, the independent addition of F270S or R1168M in Yor1p-ΔF neither modified its sensitivity to trypsin (Fig. 4*C*) nor improved its incorporation into COPII vesicles (Fig. 4*D*). Conversely, Yor1p-ΔF/F270S/R1168M at least partially restored the normal architecture, as shown by the detection of a cleavage product of ~60 kDa after incubation with trypsin (Fig. 4*C, right panel*). Similarly, the capacity for Yor1p-ΔF to populate ER vesicles was restored by the simultaneous introduction of both suppressing mutations (Fig. 4*D* and supplemental Fig. S1*D*).

Suppressing Mutations Alter the Hydrophobicity of the Transmembrane Helices—Taken together, the data described above demonstrate that F270S and R1168M are able to rescue the folding and trafficking defects associated with independent mutations in ICL1, NBD1, and ICL4. The fact that none of the suppressing mutations maps to these three domains argues against their involvement in restoring the primary lesion caused by the different misfolding mutations. The positioning of Phe-270 and Arg-1168 on the cytosolic side of TMH2 and TMH12, respectively, might indicate that these suppressing mutations could affect the insertion of TMHs within the lipid bilayer and/or influence the packing of the TMHs within the MSD-MSD interface. More comprehensive analysis of a variety of substitutions at these positions seems to corroborate this hypothesis. Reducing the hydrophobicity at position 270 (F270S, F270T, F270C, F270A, and F270G) allowed Yor1-

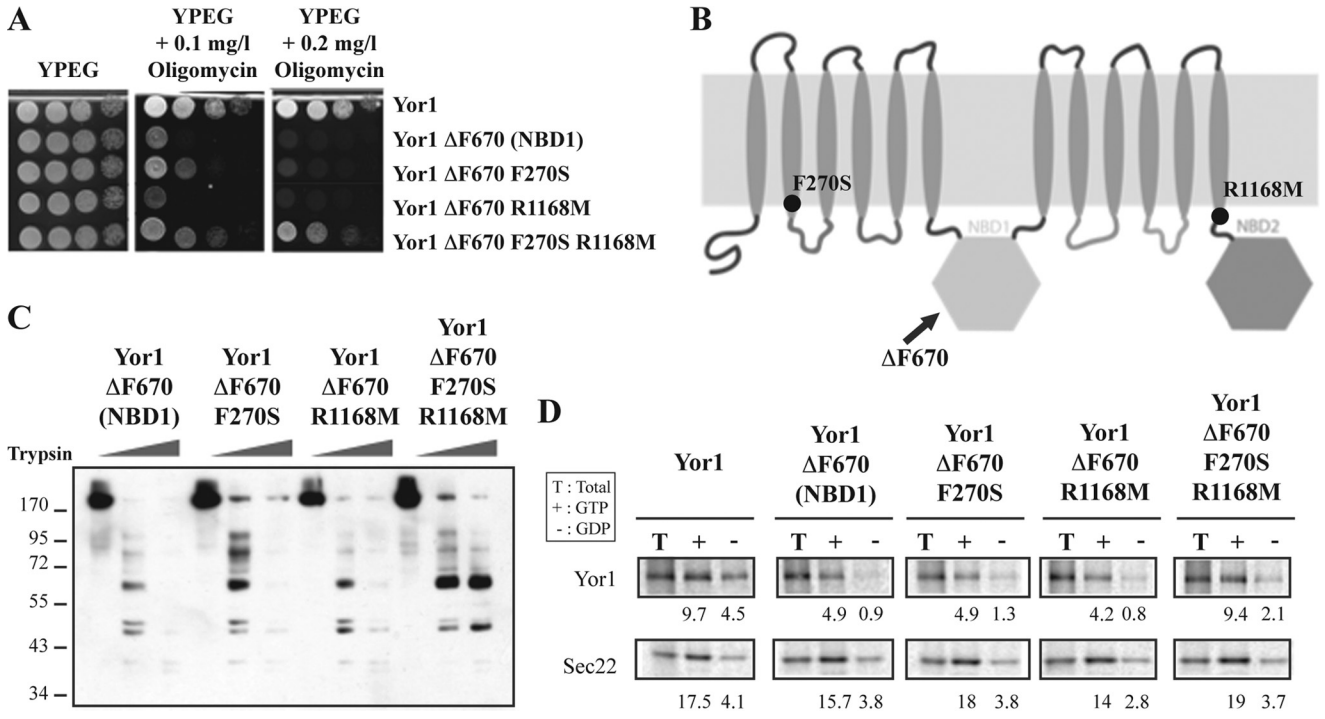

FIGURE 4. **Concurrent addition of F270S and R1168M rescues the defects associated with DF670.** *A*, the plasmids encoding the alleles indicated were transformed into a *Dyor1* strain and 10-fold serial dilutions were spotted onto YPEG or YPEG supplemented with oligomycin to test their ability to complement for drug sensitivity. Substantial resistance was observed for *YOR1-ΔF670/F270S/R1168M*. *B*, schematic map of the mutations used in Fig. 4. *C*, sensitivity to trypsin was used to test the ability of the suppressing mutations to rescue misfolding of Yor1p-ΔF670. Yor1p-ΔF670/F270S/R1168M showed increased resistance to proteolysis, whereas the digestion profile of Yor1p-ΔF670/F270S and Yor1p-ΔF670/R1168M were similar to that observed for Yor1p-ΔF670. *D*, the effect of the suppressing mutations on Yor1p-ΔF670 trafficking was tested using an *in vitro* COPII vesicle budding assay, as described in the legend to Fig. 1. Yor1p-ΔF670/F270S/R1168M showed a rate of packaging into COPII vesicles comparable with that observed for Yor1p, whereas Yor1p-ΔF670/F270S and Yor1p-ΔF670/R1168M remained poorly incorporated into vesicles similar to Yor1-ΔF670. Statistical analysis of at least three independent experiments is represented under supplemental Fig. S1*D*.

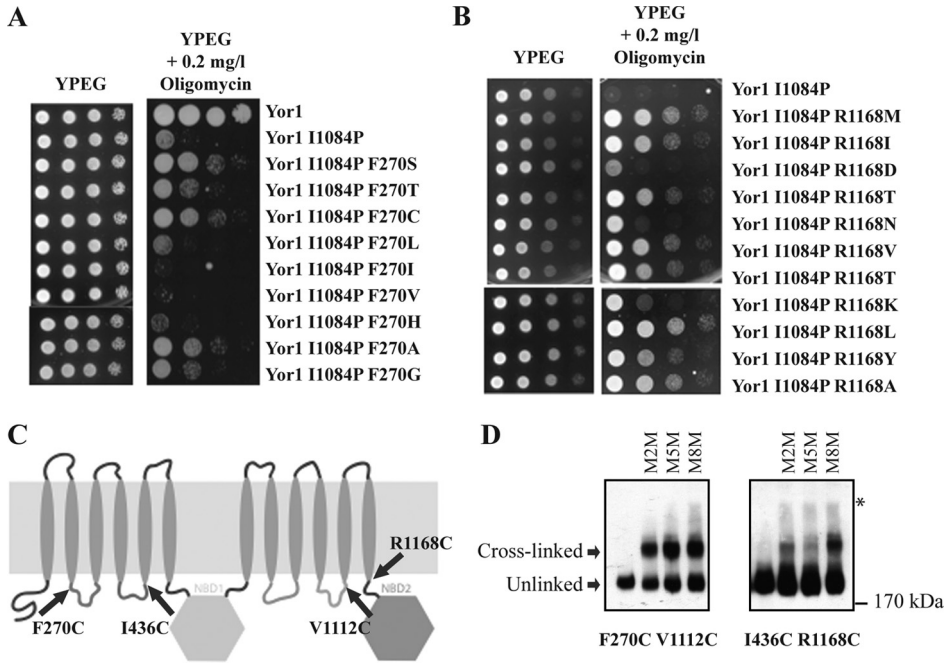

FIGURE 5. **Analysis of the influence of positions Phe-270 and Arg-1168 on Yor1p biogenesis.** Substitutions of Phe-270 (*A*) or Arg-1168 (*B*) with various amino acids were assessed for their ability to rescue the oligomycin phenotype associated with *YOR1-I1084P*. The plasmids encoding the alleles indicated were transformed into a Δ*yor1* strain and 10-fold serial dilutions were spotted onto YPEG or YPEG supplemented with oligomycin. *C*, schematic map of the positions where cysteines were introduced to conduct cross-linking experiments as presented in Fig. 4*D*. *D*, inter-domain interactions were detected by subjecting membranes containing HA-tagged cysteine-substituted mutants of Yor1p to cross-linking with M2M, M5M, or M8M, as indicated, prior to SDS-PAGE and immunoblot analysis. *Asterisk* marks the interface between stacking and resolving gels.

I1084P to regain its activity on oligomycin, whereas more conservative substitutions (F270L, F270I, F270V, and F270A) showed no effect under the same conditions (Fig. 5*A*). Conversely, substitution of Arg-1168 with any hydrophobic residue (Met, Leu, Ala, Ile, Val, Thr, and Tyr) was able to rescue the oligomycin sensitivity of *yor1-I1084*, in contrast with substitutions with charged residues (Lys, Asp, and Asn) (Fig. 5*B*).

The published structures of the prokaryotic ABC transporter exporter Sav1866 (30) and the mouse multidrug pump P-glycoprotein (15) have shed light on the organization within the membrane of the 12 TMHs that constitute the export channel of ABC transporters. By analogy with these proteins, Phe-270 of Yor1p is predicted to make close contact with the base of TMH11, whereas Arg-1168 is expected to be oriented inside the substrate pocket toward TMH5. We used *in vivo* cross-linking experi-

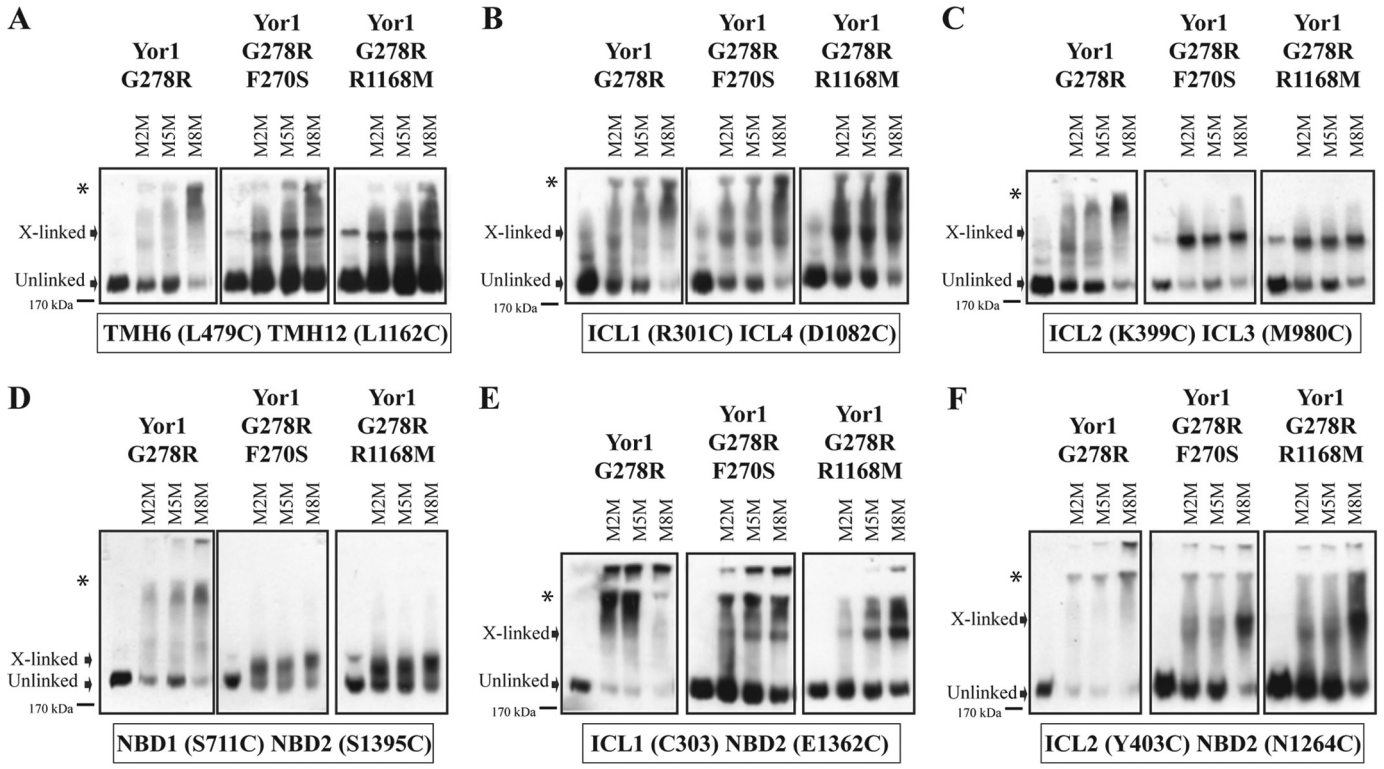

FIGURE 6. **Suppressing mutations correct multiple impaired inter-domain interfaces associated with Yor1p-G278R.** The effect of the suppressing mutations on the folding lesions presented by Yor1p-G278R was analyzed by cross-linking. Second-site mutations were able to correct the interfaces between (*A*) TMH6 and TMH12, (*B*) ICL1 and ICL4, (*C*) ICL2 and ICL3, (*D*) NBD1 and NBD2, (*E*) ICL1 and NBD2, and (*F*) ICL2 and NBD2. *Asterisk* marks the interface between stacking and resolving gels.

ments, described in Fig. 1*D*, to test these proximity models. Cysteine residues were introduced at specific positions in Yor1p (Fig. 5*C*), and the double cysteine mutants of interest (F270C/V112C and I436C/R1168C) were exposed to methanethiosulfonate cross-linkers with different spacer arm lengths: M2M (5.2 Å), M5M (9.1 Å), and M8M (13 Å). The F270C/V1112C variant showed robust cross-linking even in the presence of the shortest cross-linker M2M, suggesting a very close proximity of those two positions within the active conformation of Yor1p (Fig. 5*D*, *left panel*). Conversely, the base of TMH5 and the base of TMH12, represented by the I436C/R1168C pair, seem more distant because cross-linking was only observed in the presence of M8M and was undetectable with the shorter reagents (Fig. 5*D*, *right panel*). These results are in accord with the structural data published on Sav1866 and P-glycoprotein. As negative controls, we tested the cross-linking of single cysteine point mutants, which failed to show any cross-linked species when incubated with the longest cross-linker M8M (supplemental Fig. S3). In addition, *YOR1-F270C/V1112C* and YOR1-*I436C/R1168C* show robust complementation of the oligomycin sensitivity when transformed in a strain deleted for *YOR1*, which indicates that cysteine substitutions do not affect the function of Yor1p (supplemental Fig. S3). Together, these genetic and biochemical data suggest that F270S and R1168M might influence the folding of Yor1p by modulating the organization of the TMHs.

F270S and R1168M Restore Numerous Defective Interfaces of Yor1-G278R—We previously developed a variety of cysteine substitution pairs in *YOR1* to probe for multiple domain-domain interactions involved in shaping Yor1p. We sought to take advantage of these tools to gain more information about the contribution of F270S and R1168M in suppressing aberrant forms of Yor1p. A shown in Fig. 1*D*, the G278R mutation prevents the formation of cross-linked products between the cysteine pair L479C/L1162C, designed to inspect an interface between TMH6 and TMH12, and instead results in aggregation of the protein. This feature was observed for all the cysteine pairs tested (Fig. 6*B–F*, *left panels*), which suggests that G278R inflicts a relatively severe injury on the conformation of Yor1p and impairs the formation of numerous interfaces. Interestingly, cross-linked species could be detected after the introduction of either F270S or R1168M in the G278R/L479C/L1162C construct (Fig. 6*A*), which demonstrates that both suppressing mutations can rescue a defective assembly of TMHs. It is worth noting that residual aggregation of the suppressed constructs was still observed upon exposure with the different cross-linkers, which suggests that some of the endogeneous cysteines remain aberrantly exposed, reinforcing the conclusion that the folding rescue driven by F270S and R1168M in the context of Yor1-G278R is only partial. To assess the specificity of the folding correction generated by F270S and R1168M, we introduced the suppressing mutations in combination with G278R into additional cysteine pair substitutions that we have previously used to monitor distinct interfaces. This analysis revealed that both suppressing mutations were able to correct multiple interfaces, including ICL1-ICL4 (Fig. 6*B*), ICL2-ICL3 (Fig. 6*C*), NBD1-NBD2 (Fig. 6*D*), ICL1-NBD2

(Fig. 6*E*), and ICL2-NBD2 (Fig. 6*F*), each of which are defective in the context of the G278R mutation, indicating that each of the suppressing mutations confers a widespread ability to rescue the global conformation of Yor1p.

DISCUSSION

A large body of biochemical work has aimed to better understand the quaternary architecture of ABC transporters. Recent structural characterization of several full prokaryotic ABC transporters (14, 30) and of mouse P-glycoprotein (15) has revealed that four ICLs extend the helical structures of the transmembrane segments into the cytosol and contact the surface of NBDs to shape an MSD-NBD interface. Such an interface is predicted to transmit conformational changes between MSDs and NBDs, a fundamental aspect of the molecular mechanism employed by ABC transporters to couple substrate translocation with ATP binding/hydrolysis (9, 10). In addition, the observation that, for ABC exporters, the second ICL of one MSD contacts the opposite NBD and ICL, suggests that the contacts engaged by ICLs may be important for the harmonized response of the two halves of the protein to such conformational changes. Finally, in addition to their role in shaping an active transporter, accurate domain-domain interactions contribute to quality control during early steps of ABC transporter biogenesis; defective forms are retained in the endoplasmic reticulum to prevent their improper deployment within cells. However, the molecular determinants that govern ER retention and quality control remain largely unknown, despite their relevance as potential therapeutic targets.

We previously developed a number of tools to examine inter-domain interfaces required for the active conformation of the yeast ABC transporter, Yor1p (18, 29). We sought to exploit these biochemical approaches, combined with the genetic advantages of the yeast system, to characterize aberrant structures induced by disease-associated mutations. We show that that G278R, located in ICL1, and I1084P, located in ICL4, induce folding injuries comparable with that conferred by ΔF670, resulting in ER retention of the resulting proteins. These data support the hypothesis that impaired formation of the ICL1-ICL4-NBD1 module during biogenesis of an ABC transporter is detected by the ER quality control machinery. We identified 2 second-site mutations, F270S and R1168M, based on their ability to reverse oligomycin sensitivity associated with these aberrant proteins. These new rescuing mutations correct the folding and the ER retention of all the processing mutants investigated (Yor1p-G278R, Yor1p-I1084P, and Yor1p-ΔF). Interestingly, these second-site mutations only subtly influence the half-life of Yor1-I1084P, which argues against the hypothesis that suppression of oligomycin sensitivity is simply due to stabilization of the ER pool of the protein, which might then permit some forward traffic of the aberrant protein. Indeed, we have previously demonstrated that creating a stabilized ER pool of Yor1p-ΔF by inhibition of ER-associated degradation does not alleviate folding defects or ER retention, and also fails to restore oligomycin resistance (29). Similarly, the oligomycin sensitivity associated with either Yor1p-G278R or Yor1p-I1084P could not be rescued by down-regulation of Ubc7p, which is the major ubiquitin ligase responsible for Yor1p degradation (Ref. 29, and data not shown).

The identification of second-site mutations that suppress aberrant alleles is a useful strategy for the unbiased identification of residues involved in quaternary assembly and of structural regions that might be manipulated to restore wild-type function. Such an approach can also represent a facile way to assess the extent to which folding lesions can be corrected. We previously used this method to isolate compensatory second-site mutations that rescue the misfolding induced by a mutation located in ICL2 of Yor1p, R387G (18). Nine suppressing substitutions were clustered in three different regions of Yor1p: ICL2, the site of the original mutation, ICL3 and NBD2, which are the two domains that showed robust interactions with ICL2 by *in vivo* cross-linking experiments. The positioning of these suppressing mutations is suggestive of a restoration of a functional ICL2-ICL3-NBD2 module perturbed by the R387G mutation. Similar rescue of an inter-domain interface has recently been reported for CFTR-ΔF, where structural modeling suggested that introduction of a bulky residue in ICL4 would compensate for the missing Phe-508 of NBD1 (39). Indeed, this rationally designed second-site mutation restored trafficking to CFTR-ΔF, highlighting that correction of impaired inter-domain interfaces can be generally applicable to rescue of multiple ABC transporters.

Suppressing mutations for the misfolded ΔF-CFTR have also been isolated by genetic means using a STE6-CFTR chimera, which comprises the yeast STE6 a-factor transporter in which NBD1 has been replaced by the equivalent domain of CFTR (31–33). Remarkably, all suppressing mutations identified (I539T, G550E, R553M, and R555K) by this study are located within the NBD1 domain itself. A recent characterization of these suppressing mutations revealed that their ability to compensate for folding lesions is specific for mutations that mapped within NBD1; mutations located in other domains, including ICL4, which forms an interface with the NBD1 surface, remain dysfunctional even in the presence of the suppressing mutations (34). Furthermore, introduction of these suppressing mutations into bacterially expressed NBD1 improved the soluble protein yield (39), likely through thermodynamic stabilization of the NBD1 fold (40) Together, these data suggest that the STE6-CFTR-ΔF suppressing mutations primarily correct the original lesion in NBD1 caused by ΔF.

The corrective mutations described here likely rescue Yor1p via a mechanism distinct from either a direct rectification of the primary folding lesion or a compensatory event leading to restoration of a functional ICL1-ICL4-NBD1 module. Unlike suppressing mutations identified for CFTR-ΔF, F270S and R1168M restore the folding injury created by multiple mutations located in different domains of the protein. In addition, neither of these suppressing mutations maps to the domain containing the primary disrupting mutations or to a domain predicted to be directly involved in shaping the ICL1-ICL4-NBD1 module. Finally, the observation that F270S and R1168M restore numerous defective domain-domain interactions argues for their influence on

general properties of Yor1p folding rather than a correction of specific folding lesions. Their position relative to transmembrane helices suggests that they might modulate Yor1p folding by influencing the behavior of these hydrophobic domains relative to the lipid bilayer. Whether this modulation of transmembrane domains by F270S and R1168M affects co-translational or post-translational events of Yor1p assembly remains to be determined. Interestingly, *in vitro* studies revealed that transmembrane domains in CFTR acquire their final fold post-translationally (35). One model is that mutant forms of Yor1p adopt aberrant conformations in which packing of the TMH segments is incomplete, which in turn would be compensated by the suppressing mutations. In support of this model, Loo, Clarke, and coworkers (36–38) have found that introduction of arginine substitutions into the TMH segments can suppress folding defects caused by mutations located throughout the P-glycoprotein. An arginine residue within a TMH segment may promote TMH packing through the ability of the three polar atoms of its side chain to form H-bonds with other TMH segments. Indeed, introduction of an arginine into position 68 of TMH1 of P-glycoprotein induced hydrogen bonds with Tyr-950 and/or Tyr-953 in TMH11 (38). These results suggest that the manipulation of TMHs by corrective molecules might be a general strategy to rescue aberrant ABC transporters. In addition, the ability of a single substitution in a TMH to rescue multiple defective forms of P-glycoprotein or Yor1p might be indicative of the possible capacity for such correctors to correct diverse disease-related alleles.

The protein quality control enforced by cells to prevent exit of aberrant proteins from the ER is still poorly understood. Interestingly, the suppressing mutations described here only partially rescue the defective conformation associated with the different mutants (as determined by trypsin digest and residual aggregation upon cross-linking). This result indicates that the ERQC can overlook some folding injuries, which corroborates our earlier finding that the Yor1-R327G mutant is targeted to the plasma membrane despite the fact that this mutant presented folding lesions shared by other ER-retained mutants. Whether or not the ERQC senses a qualitative defect (specific alterations are detected, whereas others are overlooked) or a quantitative defect (a threshold of global misfolding that cannot be tolerated) remains to be determined. However, the ongoing exploration of the misfolded lesions of Yor1p, combined with intragenic and extragenic suppression strategies to search for mutants competent for trafficking of ER retained alleles of Yor1p holds great promise in elucidating the cellular mechanisms implemented during ER quality control.

Acknowledgment—We greatly appreciate the gift of plasmids pEAE83 and pEAE93 from Dr. Scott Moye-Rowley.

REFERENCES

1. Linton, K. J. (2007) *Physiology* **22,** 122–130
2. Hopfner, K. P., Karcher, A., Shin, D. S., Craig, L., Arthur, L. M., Carney, J. P., and Tainer, J. A. (2000) *Cell* **101,** 789–800
3. Smith, P. C., Karpowich, N., Millen, L., Moody, J. E., Rosen, J., Thomas, P. J., and Hunt, J. F. (2002) *Mol. Cell* **10,** 139–149
4. Chen, J., Lu, G., Lin, J., Davidson, A. L., and Quiocho, F. A. (2003) *Mol. Cell* **12,** 651–661
5. Zaitseva, J., Jenewein, S., Wiedenmann, A., Benabdelhak, H., Holland, I. B., and Schmitt, L. (2005) *Biochemistry* **44,** 9680–9690
6. Fetsch, E. E., and Davidson, A. L. (2002) *Proc. Natl. Acad. Sci. U.S.A.* **99,** 9685–9690
7. Loo, T. W., Bartlett, M. C., and Clarke, D. M. (2002) *J. Biol. Chem.* **277,** 41303–41306
8. Mense, M., Vergani, P., White, D. M., Altberg, G., Nairn, A. C., and Gadsby, D. C. (2006) *EMBO J.* **25,** 4728–4739
9. Oancea, G., O'Mara, M. L., Bennett, W. F., Tieleman, D. P., Abele, R., and Tampé, R. (2009) *Proc. Natl. Acad. Sci. U.S.A.* **106,** 5551–5556
10. Sauna, Z. E., Bohn, S. S., Rutledge, R., Dougherty, M. P., Cronin, S., May, L., Xia, D., Ambudkar, S. V., and Golin, J. (2008) *J. Biol. Chem.* **283,** 35010–35022
11. Locher, K. P., Lee, A. T., and Rees, D. C. (2002) *Science* **296,** 1091–1098
12. Hollenstein, K., Frei, D. C., and Locher, K. P. (2007) *Nature* **446,** 213–216
13. Dawson, R. J., and Locher, K. P. (2006) *Nature* **443,** 180–185
14. Ward, A., Reyes, C. L., Yu, J., Roth, C. B., and Chang, G. (2007) *Proc. Natl. Acad. Sci. U.S.A.* **104,** 19005–19010
15. Aller, S. G., Yu, J., Ward, A., Weng, Y., Chittaboina, S., Zhuo, R., Harrell, P. M., Trinh, Y. T., Zhang, Q., Urbatsch, I. L., and Chang, G. (2009) *Science* **323,** 1718–1722
16. Zolnerciks, J. K., Wooding, C., and Linton, K. J. (2007) *FASEB J.* **21,** 3937–3948
17. Serohijos, A. W., Hegedus, T., Aleksandrov, A. A., He, L., Cui, L., Dokholyan, N. V., and Riordan, J. R. (2008) *Proc. Natl. Acad. Sci. U.S.A.* **105,** 3256–3261
18. Pagant, S., Brovman, E. Y., Halliday, J. J., and Miller, E. A. (2008) *J. Biol. Chem.* **283,** 26444–26451
19. Loo, T. W., Bartlett, M. C., and Clarke, D. M. (2008) *J. Biol. Chem.* **283,** 28190–28197
20. Riordan, J. R., Rommens, J. M., Kerem, B., Alon, N., Rozmahel, R., Grzelczak, Z., Zielenski, J., Lok, S., Plavsic, N., Chou, J. L., *et al.* (1989) *Science* **245,** 1066–1073
21. Seibert, F. S., Jia, Y., Mathews, C. J., Hanrahan, J. W., Riordan, J. R., Loo, T. W., and Clarke, D. M. (1997) *Biochemistry* **36,** 11966–11974
22. Seibert, F. S., Linsdell, P., Loo, T. W., Hanrahan, J. W., Clarke, D. M., and Riordan, J. R. (1996) *J. Biol. Chem.* **271,** 15139–15145
23. Seibert, F. S., Linsdell, P., Loo, T. W., Hanrahan, J. W., Riordan, J. R., and Clarke, D. M. (1996) *J. Biol. Chem.* **271,** 27493–27499
24. Furukawa, T., Wakabayashi, K., Tamura, A., Nakagawa, H., Morishima, Y., Osawa, Y., and Ishikawa, T. (2009) *Pharm. Res.* **26,** 469–479
25. Nakagawa, H., Tamura, A., Wakabayashi, K., Hoshijima, K., Komada, M., Yoshida, T., Kometani, S., Matsubara, T., Mikuriya, K., and Ishikawa, T. (2008) *Biochem. J.* **411,** 623–631
26. Graf, G. A., Cohen, J. C., and Hobbs, H. H. (2004) *J. Biol. Chem.* **279,** 24881–24888
27. Graf, G. A., Yu, L., Li, W. P., Gerard, R., Tuma, P. L., Cohen, J. C., and Hobbs, H. H. (2003) *J. Biol. Chem.* **278,** 48275–48282
28. Delaunay, J. L., Durand-Schneider, A. M., Delautier, D., Rada, A., Gautherot, J., Jacquemin, E., Aït-Slimane, T., and Maurice, M. (2009) *Hepatology* **49,** 1218–1227
29. Pagant, S., Kung, L., Dorrington, M., Lee, M. C., and Miller, E. A. (2007) *Mol. Biol. Cell* **18,** 3398–3413
30. Dawson, R. J., and Locher, K. P. (2007) *FEBS Lett.* **581,** 935–938
31. Teem, J. L., Berger, H. A., Ostedgaard, L. S., Rich, D. P., Tsui, L. C., and Welsh, M. J. (1993) *Cell* **73,** 335–346
32. Teem, J. L., Carson, M. R., and Welsh, M. J. (1996) *Receptors Channels* **4,** 63–72
33. DeCarvalho, A. C., Gansheroff, L. J., and Teem, J. L. (2002) *J. Biol. Chem.* **277,** 35896–35905
34. He, L., Aleksandrov, L. A., Cui, L., Jensen, T. J., Nesbitt, K. L., and Riordan, J. R. (2010) *FASEB. J.* **24,** 3103–3112
35. Kleizen, B., van Vlijmen, T., de Jonge, H. R., and Braakman, I. (2005) *Mol. Cell* **20,** 277–287

36. Loo, T. W., Bartlett, M. C., and Clarke, D. M. (2006) *J. Biol. Chem.* **281,** 29436–29440
37. Loo, T. W., Bartlett, M. C., and Clarke, D. M. (2007) *J. Biol. Chem.* **282,** 32043–32052
38. Loo, T. W., Bartlett, M. C., and Clarke, D. M. (2008) *J. Biol. Chem.* **283,** 24860–24870
39. Thibodeau, P. H., Richardson, J. M., Wang, W., Millen, L., Watson, J., Mendoza, J. L., Du, K., Fischman, S., Senderowitz, H., Lukacs, G. L., Kirk, K., and Thomas, P. J. (2010) *J. Biol. Chem.* **285,** 35825–35835
40. Wang, C., Protasevich, I., Yang, Z., Seehausen, D., Skalak, T., Zhao, X., Atwell, S., Emtage, J. S., Wetmore, D. R., Brouillette, C. G., and Hunt, J. F. (2010) *Protein Sci.* **19,** 1932–1947